Electronic Supplementary Information

Alkali metal salt-assisted crystal structure switch of hybrid indium halides with near-unity photoluminescence quantum yield

Shuai Zhang, Canxu Chen, Yuanjie Chen, Bingsuo Zou*, and Ruosheng Zeng*

State Key Laboratory of Featured Metal Materials and Life-cycle Safety for Composite Structures, School of Physical Science and Technology, Guangxi University, Nanning 530004, China.

*Corresponding authors: zoubs@gxu.edu.cn; zengrsh@guet.edu.cn

Experimental section

Materials

Methylamine hydrochloride (CH_6ClN, 98%), potassium chloride (KCl, 99.8%), and indium chloride ($InCl_3$, 98%) were purchased Macklin. Antimony chloride ($SbCl_3$, 99%) was purchased from Aladdin. Hydrochloric acid (HCl, 37 wt% in water) was purchased from Sinopharm Chemical Reagent Co., Ltd. Ethanol anhydrous (CH_3CH_2OH, 99.9%) was purchased Nanning Blue Sky Experimental Equipment Co., Ltd. All of these chemical agents are used as received without further purification.

Synthesis

Fabrication of LED device

The LED device was created by integrating a NUV-LED chip (365 nm). First, the epoxy resin was mixed with 10%Sb:MA_4InCl_7 powder, mixed phase and 10%Sb:MA_2KInCl_6 powder separately. Next, the two mixtures were applied onto the LED chip's surface. Finally, the LED chip covered with the mixtures was dried in a drying oven at 70 °C for 72 hours to produce the devices.

Synthesis of Sb:MA_4InCl_7

Sb:MA_4InCl_7 was synthesized via a slow evaporation crystallization method. In a 25 mL glass bottle, 4 mmol MA, 1-x mmol $InCl_3$, and x mmol $SbCl_3$ (x = 0.005, 0.01, 0.03, 0.05, 0.1, 0.15, and 0.3) were dissolved in 4 mL of HCl. The solution was stirred magnetically at 60°C until it became

saturated, followed by filtration. The clear solution obtained after filtration was rapidly heated to 120°C and then cooled down to 60°C at a rate of 3°C/h. Slow evaporation at 60°C resulted in the formation of single crystals of Sb:MA$_4$InCl$_7$. The crystals were washed three times with ethanol and dried in an oven at 60°C for 6 hours.

Synthesis of Sb:MA$_2$KInCl$_6$

Sb:MA$_2$KInCl$_6$ was synthesized using the same slow evaporation crystallization method. In a 25 mL glass bottle, 2 mmol MA, 1.6 mmol KCl, 1-x mmol InCl$_3$, and x mmol SbCl$_3$ (x = 0.005, 0.01, 0.03, 0.05, 0.1, 0.15, and 0.3) were dissolved in 3 mL of HCl. The solution was stirred magnetically at 60°C until it became saturated, followed by filtration. The clear solution obtained after filtration was rapidly heated to 120°C and then cooled down to 60°C at a rate of 3°C/h. Slow evaporation at 60°C resulted in the formation of single crystals of Sb:MA$_2$KInCl$_6$. The crystals were washed three times with ethanol and dried in an oven at 60°C for 6 hours.

Transformation from Sb:MA$_4$InCl$_7$ to Sb:MA$_2$KInCl$_6$

Sb:MA$_4$InCl$_7$ and Sb:MA$_2$KInCl$_6$ can be synthesized using a mechanochemical grinding method too. 4 mmol MA, 0.9 mmol InCl$_3$, and 0.1 mmol SbCl$_3$ were placed in an agate mortar, and grinding with a pestle for 5 minutes yielded yellow-light-emitting 10% Sb:MA$_4$InCl$_7$. Then, adding 2 mmol KCl and continuous grinding resulted in a mixture emitting white light. Finally, adding 1 mmol InCl$_3$ and continuous grinding led to the formation of cyan-light-emitting 10% Sb:MA$_2$KInCl$_6$.

Characterization

X-ray powder diffraction (XRD, Bruker D8 Discover) was employed to characterize the phase and crystal structure. X-ray photoelectron spectroscopy (XPS, Thermo Fisher Scientific ESCALAB250Xi) was utilized for identifying the elemental composition and chemical state. The Horiba Jobin Yvon Fluorolog-3 spectrometer was used to measure steady-state photoluminescence spectra, photoluminescence efficiency, and temperature-dependent PL spectra. Time-resolved spectra were collected using the Edinburgh FLS 1000 fluorescence spectrometer. Absorption spectra were measured with the UV-VIS-NIR spectrophotometer (PerkinElmer Instruments,

Lambda750). Thermogravimetric analysis (TGA) was performed on the SHIMADZU DTG-60H by increasing the temperature from RT to 900 °C at a heating rate of 10 °C/min in a nitrogen environment. Device performance characterization was conducted using a white light LED detection system.

DFT calculations

DFT calculations were conducted using the Vienna ab initio Simulation Package (VASP) code[1] with the projection-augmented wave (PAW) method. The Perdew-Burke-Ernzerhof (PBE)[2] generalized gradient approximation (GGA) was employed as the exchange-correlation functional for structural relaxations and total-energy calculations of all structures. A cutoff energy of 350 eV and a convergence accuracy of 1×10^{-4} eV were used for the plane wave. The atomic stress convergence criterion for ion relaxation was set to be less than 0.005 eV/Å per atom. Data processing and graphical plotting were carried out using VESTA and Origin software.
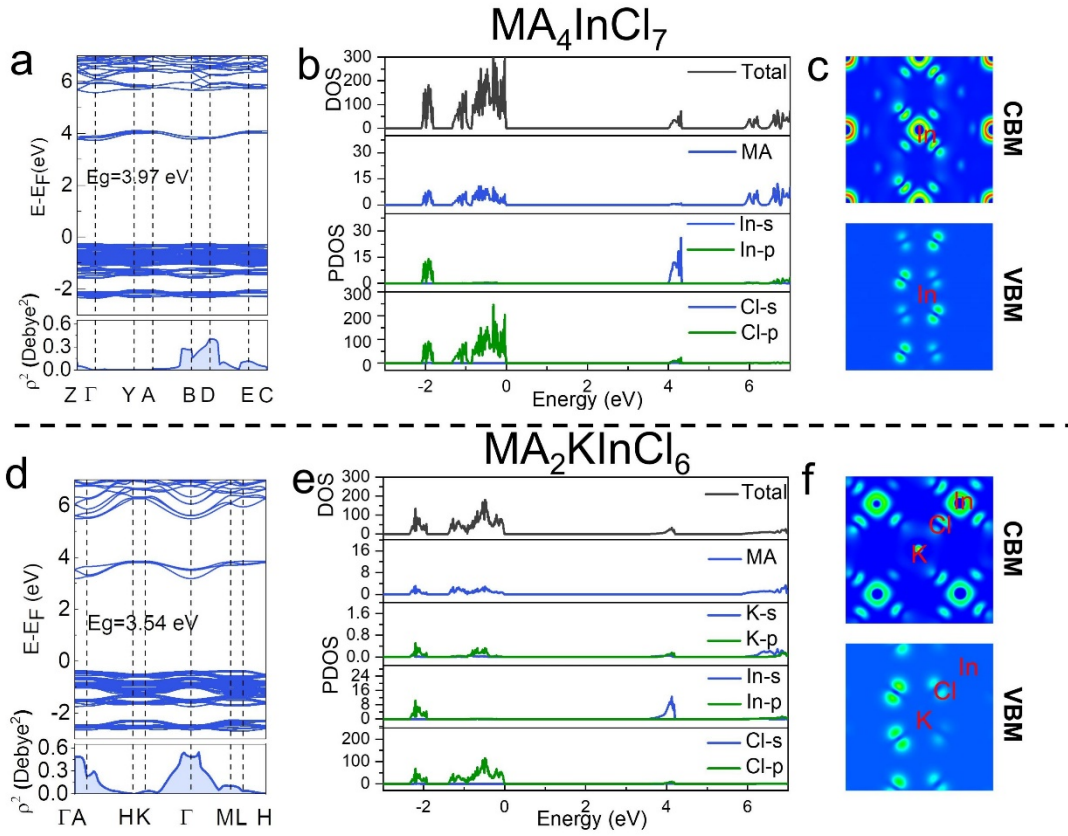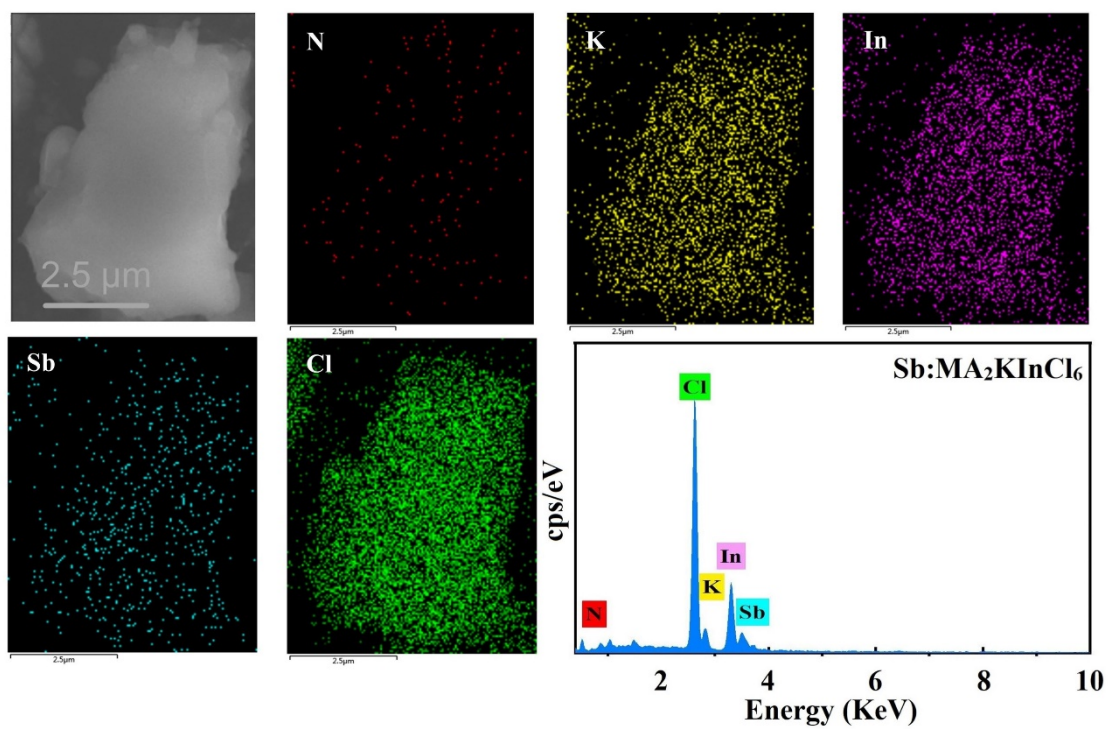
Fig. S1 Band structures (a,), density of states (b), and charge densities (c) of MA_4InCl_7. Band structures (d,), density of states (e), and charge densities (f) of MA_2KInCl_6.
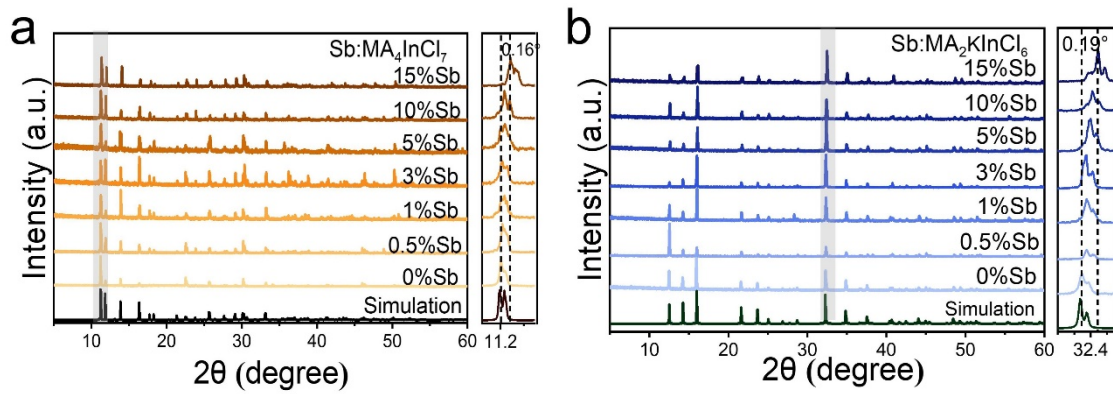
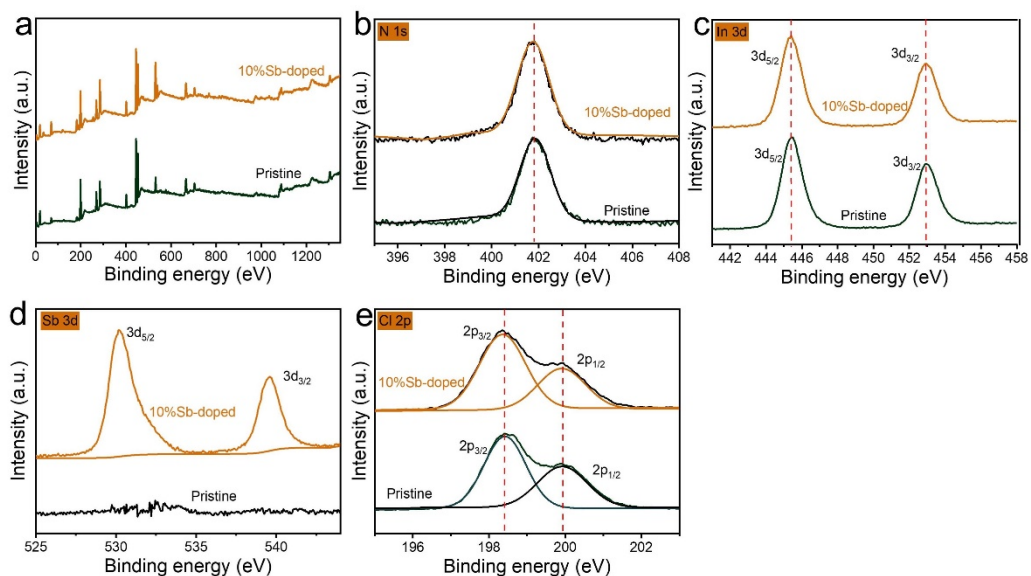**Fig. S2** XRD patterns of Sb:MA_4InCl_7 (a) and Sb:MA_2KInCl_6 (b) doped with different concentrations of Sb^{3+}.
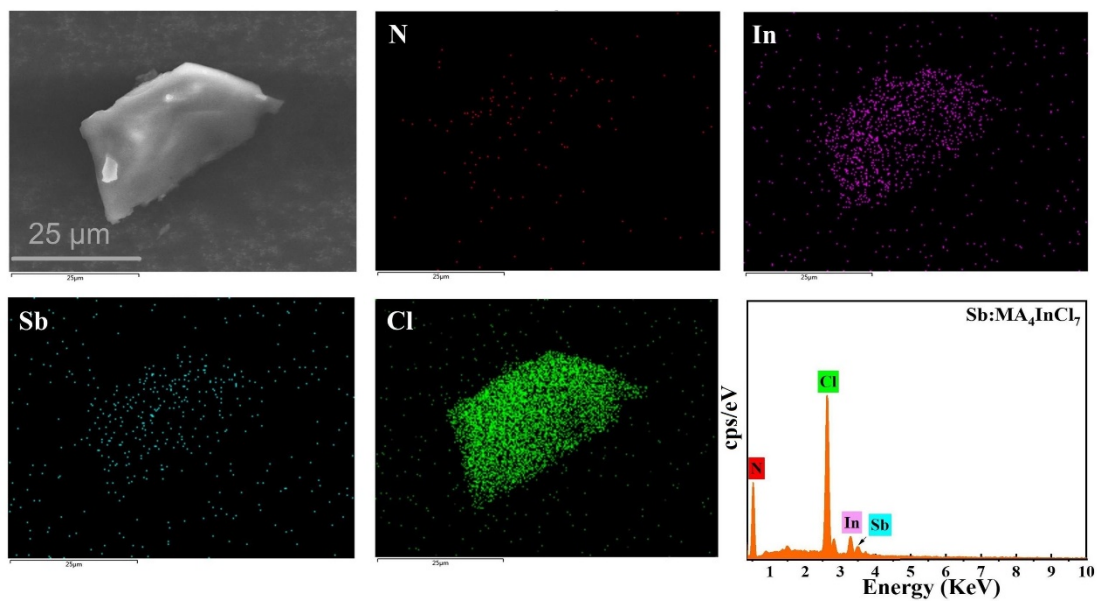
Fig. S3 EDS mapping of N, In, Sb, and Cl element of Sb:MA$_4$InCl$_7$.

Fig. S4 EDS mapping of N, K,In, Sb, and Cl element of Sb:MA$_2$KInCl$_6$.

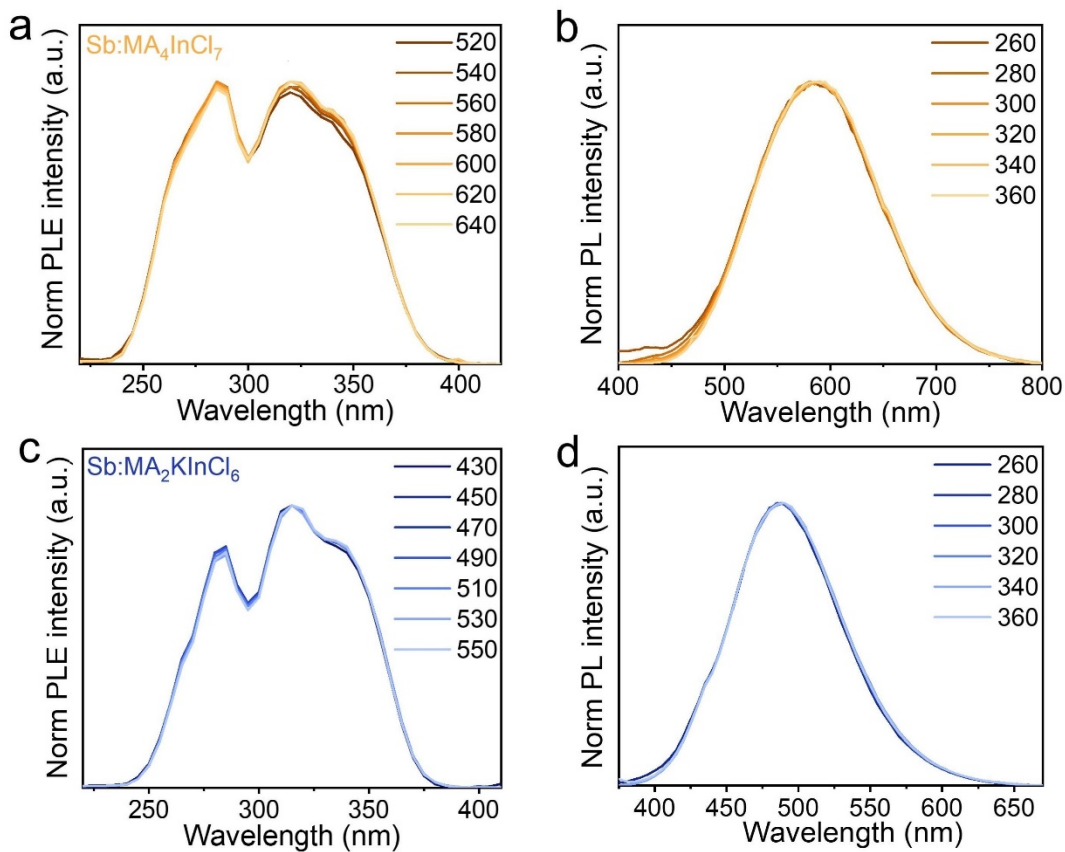**Fig. S5** (a) XPS spectrum of MA_4InCl_7 and 10% MA_4InCl_7. (b-e) High-resolution XPS spectra of N 1s, In 3d, Sb 3d and Cl 2p.
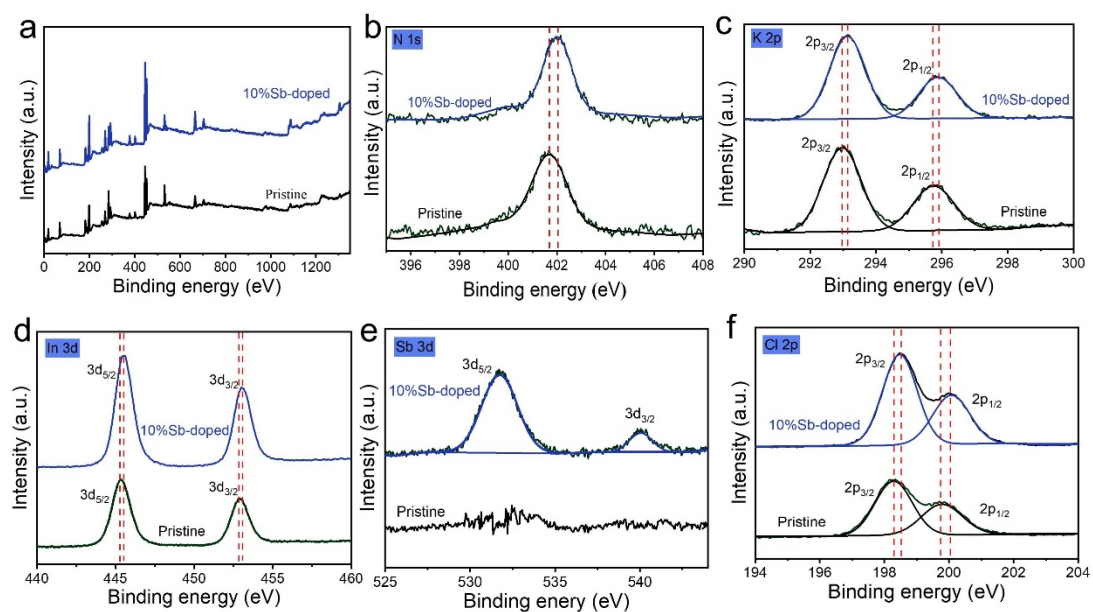
Fig. S6 (a) XPS spectrum of MA_2KInCl_6 and 10% MA_2KInCl_6. (b-f) High-resolution XPS spectra of N 1s, K 2p, In 3d, Sb 3d and Cl 2p.

Fig. S7 PL intensity of (a) Sb:MA$_4$InCl$_7$ and (b) Sb:MA$_2$KInCl$_6$ as a function of excitation powers.

Fig. S8 PLQY of Sb:MA$_4$InCl$_7$ (a) and Sb:MA$_2$KInCl$_6$ (b) doped with different concentrations of Sb.

Table S1 The PL lifetime fitting results of 0% ~ 15%Sb-doped MA$_4$InCl$_7$.

Sb^{3+}/mol%	0.5	1	3	5	10	15
τ(μs)	7.06	7.05	7.00	6.89	6.81	6.76
R^2	0.99	0.99	0.99	0.99	0.99	0.99

Table S2 The PL lifetime fitting results of 0% ~ 15%Sb-doped MA$_2$KInCl$_6$.

Sb^{3+}/mol%	0.5	1	3	5	10	15
τ(μs)	3.00	3.01	2.97	2.87	2.68	2.60
R^2	0.99	0.99	0.99	0.99	0.99	0.99

Fig. S9 PLE spectra (a) and PL spectra (b) of Sb: MA_4InCl_7 at different excitation wavelengths; PLE spectra (c) and PL spectra (d) of Sb: MA_2KInCl_6 at different excitation wavelengths.

Table S3 The bond lengths and bond angles data of Sb-doped MA_4InCl_7 structure at 0, 80, 100, 200,

300, and 400K.

Sb-doped MA$_4$InCl$_7$		0K	80K	100K	200K	300K	400K
Bond length(Å)	Sb1-Cl13	2.54024	2.55419	2.65605	2.66706	2.47176	2.67559
	Sb1-Cl14	2.54024	2.63445	2.56839	2.58004	2.67497	2.86234
	Sb1-Cl17	2.55783	2.57883	2.57491	2.56849	2.57347	2.57113
	Sb1-Cl18	2.55783	2.67359	2.66539	2.70751	2.73053	2.66677
	Sb1-Cl21	2.55788	2.58502	2.67357	2.6457	2.93019	2.69308
	Sb1-Cl22	2.55794	2.6307	2.65538	2.46432	2.78299	2.77101
Band angles(°)	Cl13-Sb1-Cl17	90.2231	86.4625	91.9172	91.3514	92.5547	104.5111
	Cl13-Sb1-Cl18	89.7769	97.1232	95.182	101.9801	97.2061	79.0805
	Cl13-Sb1-Cl21	88.9039	88.1263	91.0542	79.1399	100.6001	100.0175
	Cl13-Sb1-Cl22	91.0963	88.102	85.0439	91.3396	84.8746	78.9678
	Cl14-Sb1-Cl17	89.7769	88.7554	89.23	81.883	92.2096	93.9395
	Cl14-Sb1-Cl18	90.2231	87.4637	83.3848	84.6293	78.1379	83.2136
	Cl14-Sb1-Cl21	91.0961	89.2054	102.482	94.6802	85.4852	82.0855
	Cl14-Sb1-Cl22	88.9037	94.2261	81.3846	94.4368	88.657	97.6995
	Cl17-Sb1-Cl21	88.8392	86.2543	92.1473	86.1387	90.4565	90.9556
	Cl17-Sb1-Cl22	91.1619	89.5378	89.3006	91.1206	94.333	92.8521
	Cl18-Sb1-Cl21	91.1608	89.3961	89.7863	94.1199	87.2928	78.773
	Cl18-Sb1-Cl22	88.8381	95.0242	89.2601	90.7853	87.0378	97.4222

Table S4 The bond lengths and bond angles data of Sb-doped MA$_2$KInCl$_6$ structure at 0, 80, 100, 200, 300, and 400K.

| Sb-doped MA$_2$KInCl$_6$		0K	80K	100K	200K	300K	400K
Bond length(Å)	Sb1-Cl3	2.52474	2.80609	2.79592	2.8968	2.79063	2.69388
	Sb1-Cl6	2.53766	2.68327	2.63658	2.8359	2.69198	2.75503
	Sb1-Cl9	2.53134	2.55521	2.73003	2.5876	2.662	2.59735
	Sb1-Cl10	2.55406	2.58951	2.59906	2.48828	2.73268	2.73358
	Sb1-Cl13	2.55717	2.6918	2.64585	2.57604	2.71956	2.58477
	Sb1-Cl16	2.5697	2.6272	2.70363	2.57961	2.66105	2.75196
Band angles(°)	Cl3-Sb1-Cl6	92.2389	95.3678	90.7192	86.3066	98.5961	88.5557
	Cl3-Sb1-Cl9	92.6564	92.6767	85.1857	96.1995	94.9449	86.3222
	Cl3-Sb1-Cl13	89.7584	83.4657	90.9989	90.3762	81.8804	97.7936
	Cl3-Sb1-Cl16	86.9198	82.7375	86.5848	88.7675	72.9384	87.7269
	Cl6-Sb1-Cl9	91.6907	95.5413	96.0209	86.5799	80.9247	89.6176
	Cl6-Sb1-Cl10	89.9129	87.8167	87.5648	89.3689	104.637	91.5465
	Cl6-Sb1-Cl13	87.3661	87.0786	84.2912	85.6002	104.3259	84.6076
	Cl9-Sb1-Cl10	86.6811	86.7387	86.4111	83.0492	88.8986	84.1618
	Cl9-Sb1-Cl16	90.2902	87.6301	96.0209	89.2593	85.406	82.8346
	Cl10-Sb1-Cl13	90.9373	96.9889	97.4132	89.7692	92.1401	91.6896
	Cl10-Sb1-Cl16	90.9498	94.0968	95.6561	95.5023	84.5813	90.9128
	Cl13-Sb1-Cl16	90.6858	89.6485	92.0338	99.1685	88.9878	103.1564
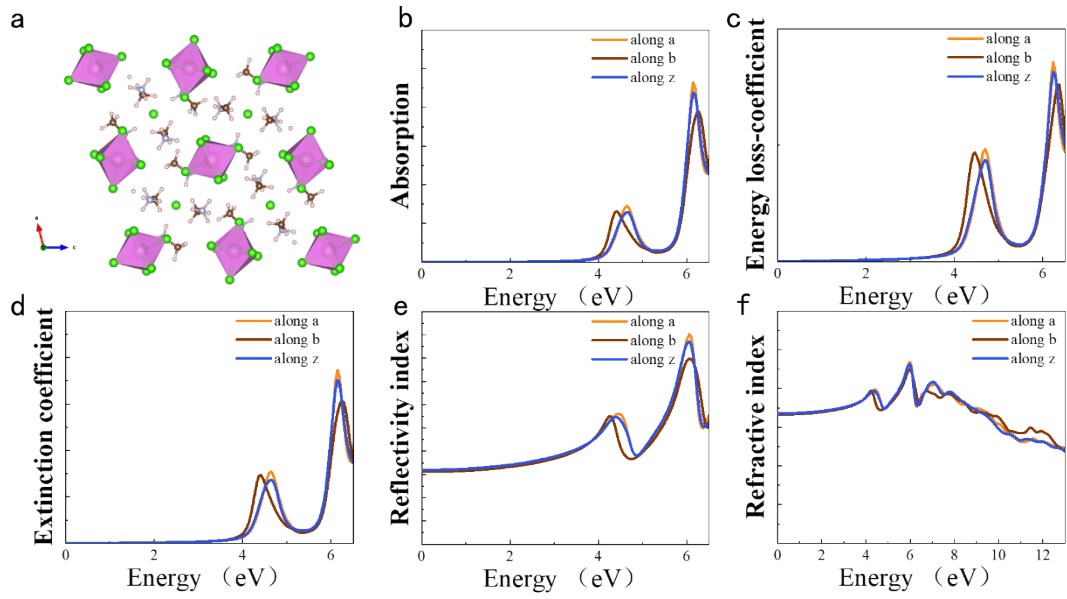
Fig. S10 (a) Crystal structures of MA_4InCl_7; (b-c) absorption, energy loss coefficient, extinction coefficient, reflectivity index and refractive index of pristine MA_4InCl_7.
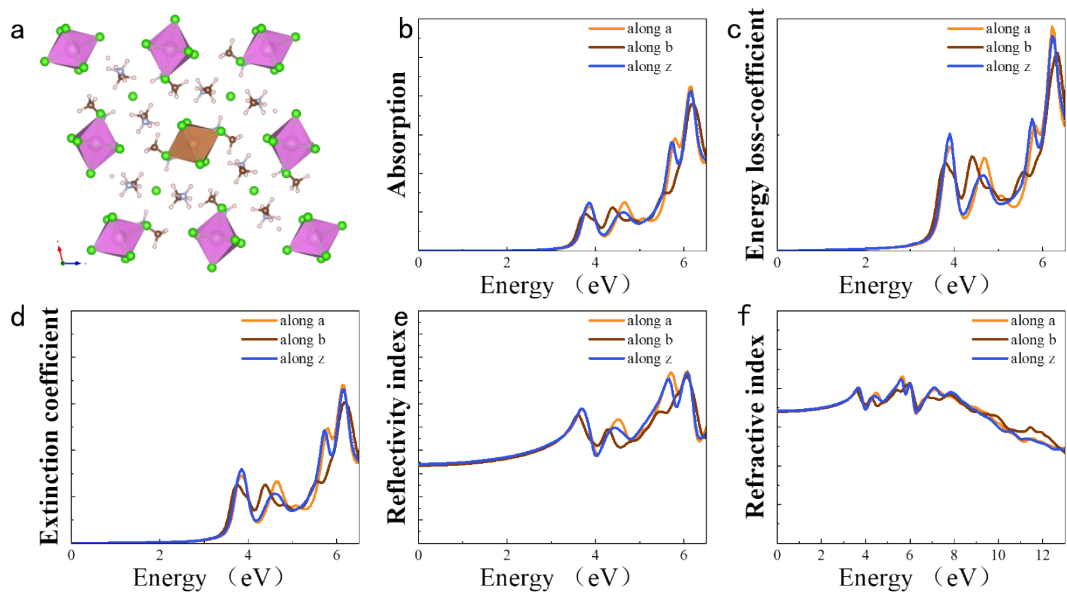

Fig. S11 (a) Crystal structures of $Sb:MA_4InCl_7$; (b-c) absorption, energy loss coefficient, extinction coefficient, reflectivity index and refractive index of pristine $Sb:MA_4InCl_7$.
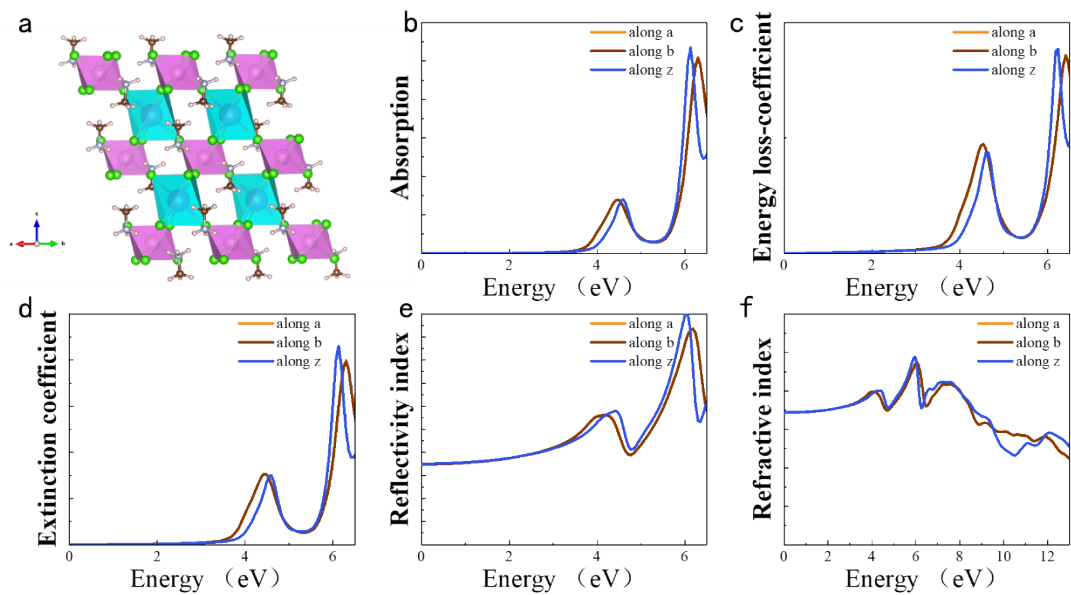
Fig. S12 (a) Crystal structures of MA$_2$KInCl$_6$; (b-c) absorption, energy loss coefficient, extinction coefficient, reflectivity index and refractive index of pristine MA$_2$KInCl$_6$.
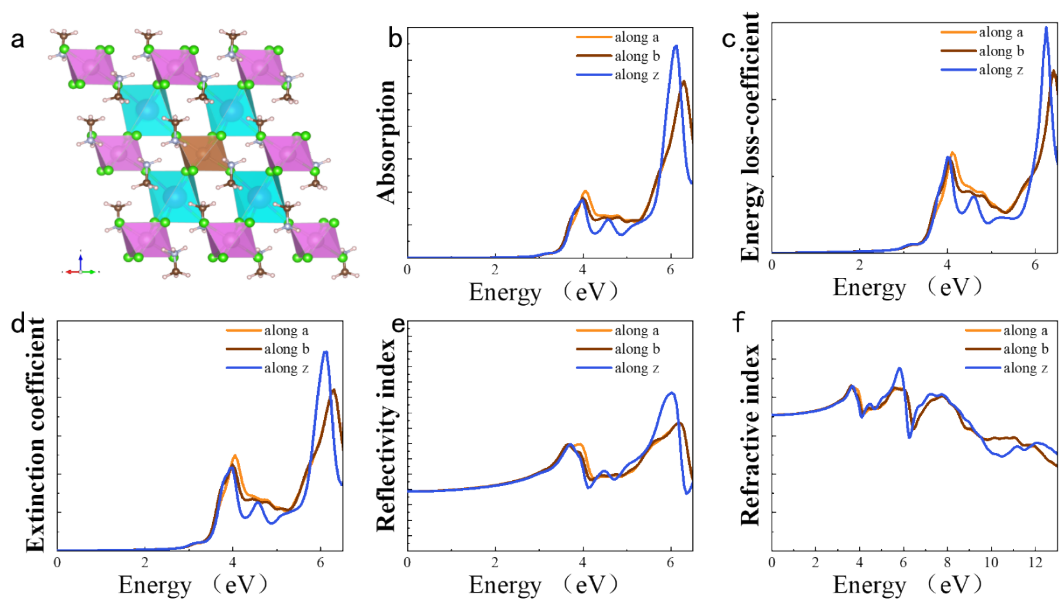
Fig. S13 (a) Crystal structures of Sb:MA$_2$KInCl$_6$; (b-c) absorption, energy loss coefficient, extinction coefficient, reflectivity index and refractive index of pristine Sb:MA$_2$KInCl$_6$.
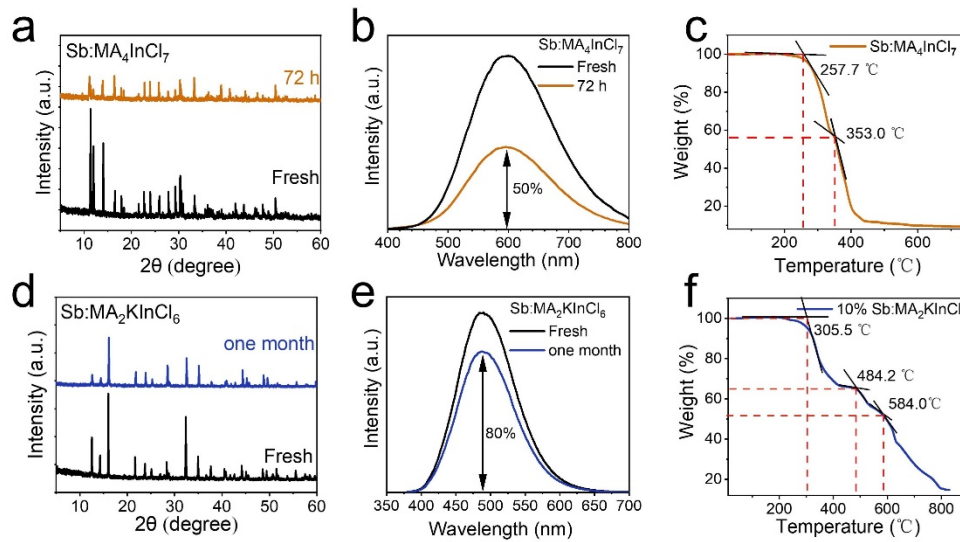
Fig. S14 Structure and PL stability in air, XRD patterns, PL spectra, and thermogravimetric analysis curves of 10%Sb:MA$_4$InCl$_7$ (a-c) and 10%Sb:MA$_2$KInCl$_6$ (d-f).

Reference

[1] G. Kresse, J. Furthmuller, Phys Rev B Condens Matter 1996, 54, 11169.

[2] J. P. Perdew, K. Burke, M. Ernzerhof, Phys Rev Lett 1996, 77, 3865.